IOP Conf. Series: Materials Science and Engineering **319** (2018) 012065 doi:10.1088/1757-899X/319/1/012065

Stress analysis on the reinforcement particles of the metal matrix composite by Raman spectroscopy

A K M Asif Iqbal[1], Yoshio Arai[2]

[1]Faculty of Manufacturing Engineering, University Malaysia Pahang, 26600, Pekan, Pahang, Malaysia.
[2]Division of Mechanical Engineering and Science, Graduate School of Science and Engineering, Saitama University, 338-8570, Japan.

asifiqbal@ump.edu.my

Abstract. In this research, the stress state of the reinforcing SiC particles in a hybrid MMC is investigated by micro Raman spectroscopy. The experiment was carried out *in situ* in the Raman spectroscopy. Experimental results show that cracks due to monotonic loading propagates by the debonding of the particle/matrix interface and particle fracture. Moreover, secondary cracks form in front of the main crack tip coalesce with the main crack in subsequent loading and final failure occurs. A high decrease in stress (several hundred in MPa) is observed with the interfacial debonding at the interface and with the particle fracture on the particle. The critical tensile stresses for particle-matrix interface debonding and particle fracture develop in hybrid MMC are also estimated during the crack propagation.

1. Introduction

Nowadays, aluminium based MMCs have made a substantial research interest due to their improved mechanical properties compared to conventional engineering materials [1-3]. The incorporation of the reinforcement particles, such as SiC and Al_2O_3 particles to conventional aluminium alloys exceptionally increases its modulus and fracture resistance. Therefore, these materials are now particularly attractive for structural and wear applications [3]. However, these materials show relatively poor fracture properties as they become often brittle once the higher volume fraction of reinforcement is added to them [4]. Previous studies explained that the key mechanism of the fracture of MMCs is the huge differences in strain carrying capability of reinforcement and the matrix alloy as the reinforcement deforms elastically and the matrix deforms plastically [5–7]. Due to the constrained plastic flow in the matrix that exists between the reinforcement particles in the MMCs, hydrostatic stresses develop which plays a significant role in the failure mechanism during monotonic and cyclic deformations [8]. Among the different constraint level, interfacial bonding between reinforcing particles and matrix alloy becomes a dominating factor in local failure processes and the strengthening of MMCs. A good bonding in the interface results high dislocation density in the matrix which improves the strength of MMC [9]. Besides, the damage initiation mechanism in the different types of MMCs has been broadly investigated and found that the damage often starts due to the interface debonding of the reinforcement and matrix [10, 11]. Iqbal et al. [11] have investigated the fatigue fracture initiation and propagation mechanism in the hybrid MMC and observed that the fracture was initiated by the debonding of particle and matrix located in the hybrid clustering region. The initiated microcracks coalesced to the nearby microcracks in front of the crack tip and propagated through the reinforcement-matrix interface. This phenomenon

Table 1. Chemical composition of AC4CH alloy, (wt%)

Si	Fe	Mg	Ti	Al
7.99	0.2 (max.)	0.57	0.07	Bal.

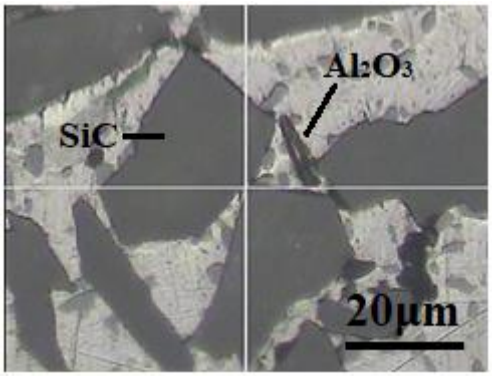

Figure 1. Microstructure of hybrid MMC

was also investigated numerically and found that high level of stress concentration occurred on the particle-matrix interface and the area is highly vulnerable to fracture initiation [12, 13]. Usually, the crack propagation occurs in two ways, partial debonding and reinforcement breakage. In case of reinforcement partial debonding, the crack propagates along the reinforcement–matrix interface while the reinforcement breakage occurs when the reinforcement fails as the load exceeds the reinforcements tensile strength [14]. It is observed that if the interfacial crack spreads far enough, the connecting reinforcement breaks finally, after the reinforcement-matrix interfacial debonding. Therefore, it would be very important to know the stress state of the reinforcing particles during the crack propagation as materials reliability in service depends on it.

Micro-Raman spectroscopy (MRS) is a potential tool in experimental mechanic's field as this technique provides some unique benefits, for example, non-destructive, non-contact, high spatial resolution and depth focus. This technique is also very useful to measure the distribution of the stress or strain on the reinforcement at microscale [15]. MRS has widely been used to study the load transfer behaviour of reinforcement debonding, bridging, pull-out and fracture [16]. In the present study, micro Raman spectroscopy is used to analyze the stress developed in the reinforcement particles during crack propagation in a hybrid MMC. The reinforcement fracture and the interfacial fracture are also observed in this study.

2. Materials and experimental procedures

Hybrid metal matrix composite with 21 Vol% SiC particles and 9 Vol% Al_2O_3 whiskers as reinforcements and the aluminium alloy JIS-AC4CH as matrix is used for this study [17]. The MMC material is fabricated by the squeeze casting process. The maximum casting pressure is used to 100 MPa. The squeeze casting pressure of 100 MPa is adequate to overcome the resistance against the flow and to press the melt into all the open pores of the hybrid preform. Finally, the material is heat treated using the T7 process. The chemical composition of AC4CH alloy is listed in Table 1. The microstructure of the hybrid MMC is shown in figure 1. The SiC particles in the hybrid MMC are mostly rectangular with sharp corners, and the Al_2O_3 whiskers are roller-shaped. The average length of SiC particles and the Al_2O_3 whiskers is 23 μm and 35 μm respectively. The average diameter of the Al_2O_3 whiskers is 2 μm. The mechanical properties of reinforcement materials and hybrid MMC are shown in Table 2.

Table 2. Mechanical properties of reinforcement and tested materials

Parameters	Al_2O_3	SiC	Al alloy	Hybrid MMC
Young's modulus (GPa)	380	450	70.0	142
Poisson's ratio	0.27	0.20	0.33	0.28
Yield strength (MPa)	-	-	131	166
Tensile strength (MPa)	-	-	262	228
Tensile elongation (%)			9.22	2.77

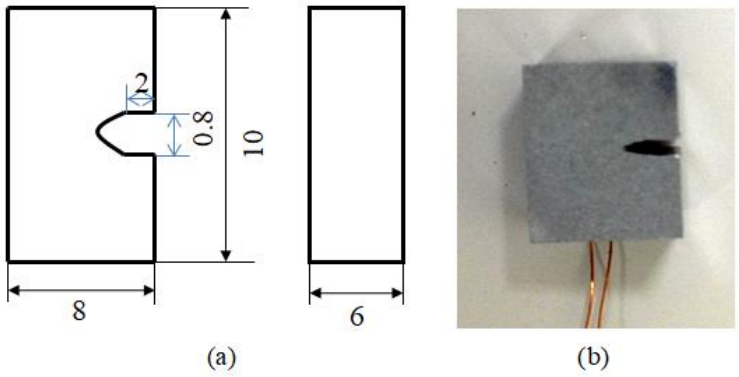

Figure 2. Specimen used in the experiment (a) schematic illustration of dimension, (b) original specimen

A rectangular notched specimen is used for the experiment as shown in figure 2. The machined surfaces of the specimens are polished by using a polishing machine with 15, 3, and 1 μm diamond particles sequentially until all scratches and surface machining marks are removed and become smooth enough to prevent attenuation of the scattered light from the specimen. The experiment is carried out *in situ* in the Raman spectroscopy with special loading fixture consists with a wedge and a mechanical actuator. A schematic illustration of the experimental setup is shown in Fig. 3. By rotating the screw in the fixture, the wedge moves towards the notch which provides crack face opening of the specimen. The wedge angle is 5.4 deg. The rotation of the screw is manually controlled and monitored carefully. The data presents in this article are in relation with the rotation of the screw in the fixture. A strain gauge is attached at the bottom of the specimen to determine the contact of the wedge to the specimen notch. The strain data is recorded by a computer data acquisition system. All tests are carried out at room temperature. The initiation and propagation of micro-cracks are observed by the optical microscope attached in the micro Raman spectroscopy.

2.1. Raman spectroscopy measurement

The Raman microscopic analysis is carried out on a laser micro-Raman spectrometer (Lamda vision LV-RAM 532). A green laser with a wavelength of 532 nm and a power of 70 mW is used. The laser beam is focused to a 2μm diameter spot on the specimen surface using an optical microscope with X50 objective lens. The backscattered light is dispersed by leading it to the spectrometer through the microscope objective. Raman spectra are recorded using a charge coupled device (CCD). The Raman frequencies of the Raman bands are obtained with an accuracy of $\pm 0.5 cm^{-1}$.

3. Results and Discussion

To analyze the stress concentration on the reinforcing particles, first, the Raman gage factor of SiC particle is determined. Therefore, an axial compressive load of 200 N is applied to a small SiC bar and Raman peaks are observed. The gage factor (GF) is calculated to be 0.0023 cm-1.

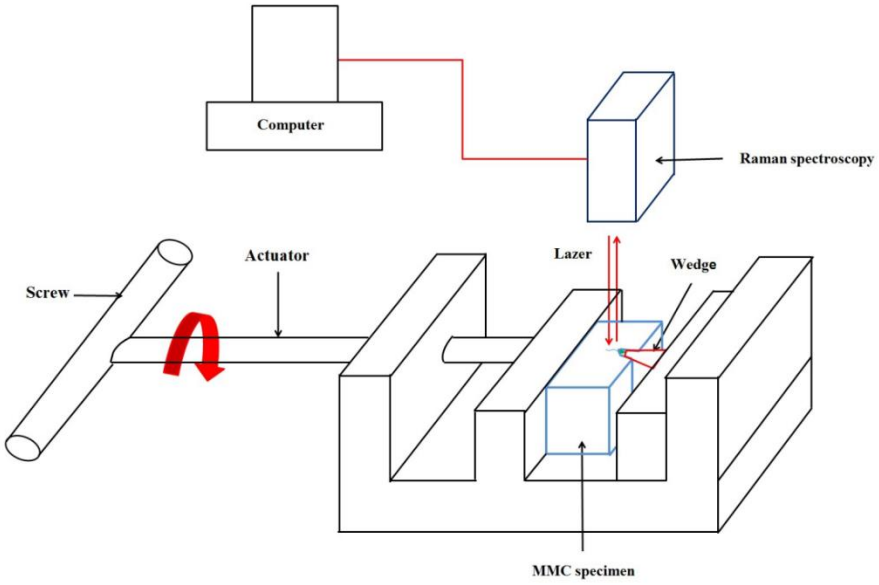

Figure 3. Schematic illustration of experimental setup

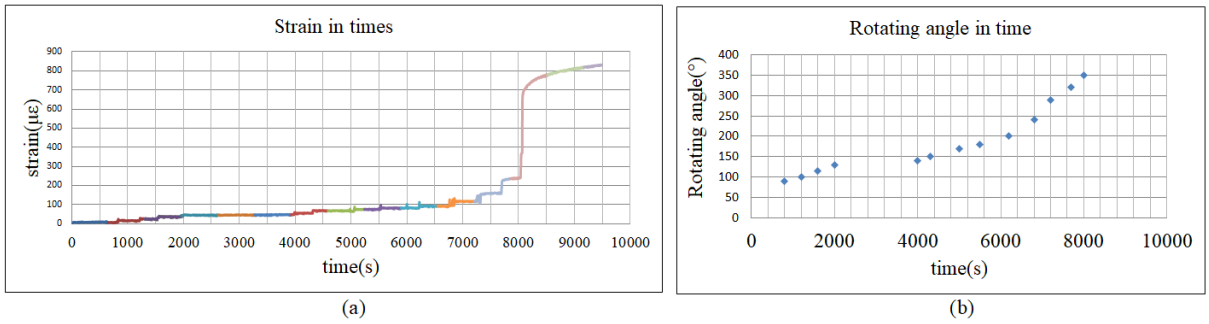

(a) (b)

Figure 4. (a) Change of strain in different times, (b) Rotation of screw in different times.

The change in strain in different times and with different angles of the rotating screw is presented in Figure 4. The crack nucleation at the notch during the application of monotonic load as a sudden increase of the strain is shown in the figure 4. The screw is rotated to 300º from 0 to 7000s (Fig. 4b), however, no substantial change in strain is found. This indicates that the wedge did not touch the notch at this stage. The strain starts increasing at 7700 s and 320º rotation of the screw, indicating the contact of the wedge to the notch. Besides, at 8000 s and 360º rotation of the screw, the strain increases rapidly, indicating the crack initiation at the tip of the notch at this stage. This result clearly demonstrates that the crack initiates at 40º increment in rotation of the screw from the absolute value of rotation angle 320º at which the wedge contacts the notch. In the following discussion, we use the increment value in rotation from the 320º and call it 'rotation angle'. To determine the state of the stress and the state of crack propagation, Raman spectrum is taken on several particles in different loading angle. One of the particles has been chosen for this paper is particle 8. The optical micrograph of the particle 8 in different rotating angle and the behaviour of a propagating crack at the interface between particle 8 and matrix alloy is shown in the figure 5. The red spots on the particle indicate the Raman laser spots. Initially, no

cracks are observed at the interface of the particle (Fig. 5a). Besides, at 45º rotation of the screw (Fig. 5b), the main crack propagates along the interface of the particle as indicated in the Fig 5b. At the same time, another crack is observed in front of the main crack tip (as indicated by the arrow in Fig 5b). The presence of arrested crack at this stage indicates the interface debonding seems to be stable. The crack then further propagates by deflecting into SiC particle at the 50º rotation of the screw (Fig. 5c). The particle fracture is observed once the rotation of the screw reached to the 55º angle (Fig. 5d).

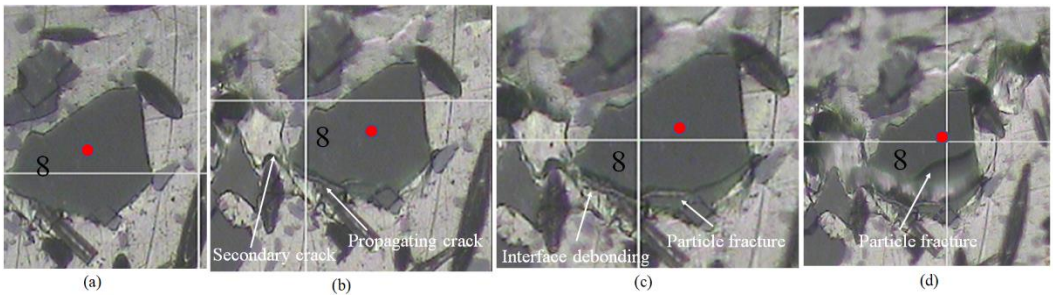

Figure 5. Interface crack on particle at different rotating angle of the screw.

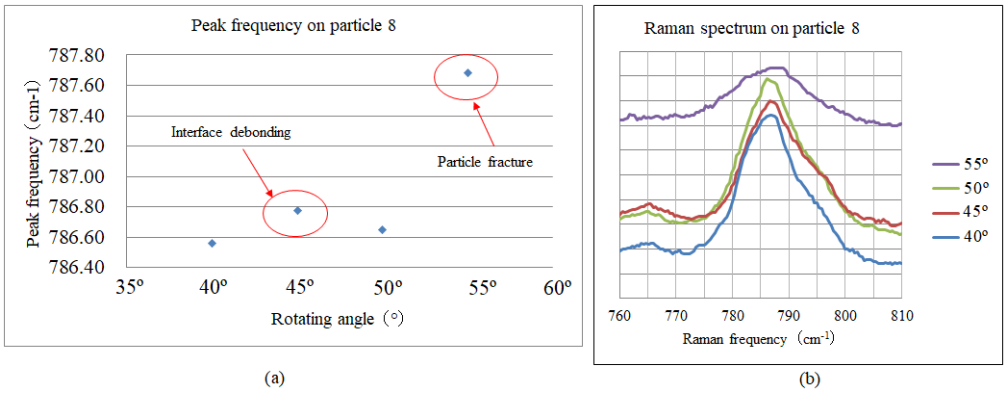

Figure 6. Raman spectroscopy on particle 8 in different rotating angle (a) peak wave number (b) Raman spectrum

Table 3. Change of accumulated stress on particle 6 in different rotating angle

Rotating angle (°)	Peak wave number (cm^{-1})	Change in stress (MPa)	Accumulated change in stress (MPa)
40	786.56		
		-435	
45	786.77		-435
		-146	
50	786.65		-581
		-245	
55	787.7		-826

The same phenomena are also observed in other particles lies in the crack propagation direction. Figure 6 represents the results of the Raman spectrum taken on the particle 8 in different rotating angle. At the angle of 45º, the peak value of Raman spectrum is found to be 786.77 cm-1. At this stage, interfacial debonding occurs at particle 8. The Raman spectrum also moves to higher peak value when the crack deflects into the particle at 50º rotation. Besides, the highest value of the Raman spectrum is found to be 787.7 cm-1 at 55º rotating angle. At this stage particle 8 becomes fractured. From the obtained peak wave number, the change in stress for debonding to take place in particle 8 is calculated

by using the SiC gage factor and the result is presented in Table 3. The stress concentration on the particle 8 is calculated to be -435 MPa (- sign indicates a decrease in stress) once the particle is debonded from the matrix. The decrease in stress compared to the un-cracked state means an unloading of originally tensile stress develops due to the opening of the crack under wedge loading. The change in stress due to crack deflection from the interface to the SiC particle is -146 MPa. Besides, the maximum change in stress measured in the particle 8 after particle fracture is found to be -245 MPa at the angle of 55º of the screw. The accumulated change in stress from the un-cracked state to the particle fracture is -826 MPa which means 826 MPa is the estimated value of tensile stress developed in the particle located just ahead of the crack tip before fracture. The similar high value of change in stress is also measured in other particles in front of the crack tip.

The above results clearly show that the crack due to the waged-type monotonic load propagates along the interface of particle-matrix as well as through the particle in the hybrid MMC. The local effective stress, which is acting on the particle ahead of the crack tip reaches extremely high values (800 – 900 MPa). At the fracture stress under monotonic loading condition, the reinforcing particles deformed elastically within the plastically deforming matrix alloy. Thus, a large strain mismatch occurs between these two materials. For this mismatch of strain, a consequent concentration of stress is generated in the particles and at the interface between the reinforcing particles and matrix alloy. These stresses cause the interface separation of particle-matrix as well as the particle fracture, and the crack propagates till the final failure occur.

4. Conclusions

The stress state of the reinforcing particles in hybrid MMC has been investigated by *in situ* fracture experiment in the micro Raman spectroscopy. The results show that the cracks developed due to the wedge type monotonic load propagates by the debonding of the particle/matrix interface and particle fracture. Secondary cracks also generate in front of the main crack tip, which coalesce with the main crack and the final failure occurs. The Raman spectroscopy confirms that stress drops rapidly (several hundred in MPa) once the interfacial debonding and particle fracture occur.

Acknowledgement

The authors express gratitude to the University Malaysia Pahang for providing financial support to present the paper at the conference under RDU 150350.

References.

[1] Clyne TW, Withers PJ. An introduction to metal matrix composites. Cambridge University Press, Cambridge; 1993.
[2] Chawla KK. Composite materials—science and engineering. Springer-Verlag, New York; 1987.
[3] Suresh S, Mortensen A, Needleman A. Fundamentals of metal matrix composites. Butterworh / Heinemann, London; 1993.
[4] Miserez A, Rossoll A, Mortensen A. Investigation of crack-tip plasticity in high volume fraction ceramic particle reinforced metal matrix composites. Eng Fract Mech 2004;71:2385–406.
[5] Levin M, Karlsson B. Influence of SiC particle distribution and prestraining on fatigue crack growth rates in aluminium AA 6061–SiC composite material. Mater Sci Technol 1991; 7: 596–607.
[6] Davidson DL. Fatigue and fracture toughness of aluminium alloys reinforced with SiC and alumina particles. Compos 1993;24:248–55.
[7] Chen AL, Arai Y, Tsuchida E. A numerical study on the effect of thermal cycling on monotonic response of cast aluminium alloy-SiC particulate composites. Theor Appl Mech 2004;53:63–73.
[8] Chawla N, Andres C, Jones JW, Allison JE. Effect of SiC volume fraction and particle size on the fatigue resistance of a 2080 Al/SiCp composite. Metall Mater Trans A 1998;29:2843–54.
[9] Chen EY, Lawson L, Meshii M. The effect of fatigue microcracks on rapid catastrophic failure in Al–SiC composites. Mater Sci Eng A 1995;200:192–206.

[10] Chen ZZ, Tokaji K. Effects of particle size on fatigue crack initiation and small crack growth in SiC-particulate reinforced aluminium matrix composites. Mater Lett 2004;58:2314–21.
[11] Iqbal AA, Arai Y, Araki W. Effect of Hybrid Reinforcement on Crack Initiation and Early Propagation Mechanisms in Cast Metal Matrix Composites during Low Cycle Fatigue. Mater Des 2013;45:241-52.
[12] Yan YW, Geng L, Li AB. Experimental and Numerical Studies of the Effect of Particle Size on the Deformation Behavior of the Metal Matrix Composites. Mater Sci Eng A 2007;448:315-25.
[13] Iqbal AA, Arai Y, Araki W. Effect of Reinforcement Clustering on Crack Initiation Mechanism in a Cast Hybrid Metal Matrix Composite during Low Cycle Fatigue. Open J compos mater 2013:3:97-106.
[14] Zhenkun L, Wang Quan, Qiu W. Micromechanics of fiber–crack interaction studied by micro-Raman spectroscopy:Broken fiber. Opt Laser Eng 2013;51:1085-91
[15] Lei ZK,QiuW, Kang YL, Liu G,Yun H. Stress transfer of single fiber/micro droplet tensile test studied by micro-Raman spectroscopy. Compos A 2008;39:113–8.
[16] Lei ZK,Wang Q, Kang YL, Qiu W, Pan XM. Stress transfer in microdroplet tensile test:PVC coated and uncoated Kevlar-29 single fiber. Opt Laser Eng 2010;48:1089–95.
[17] “Aluminium Alloy Castings,” JIS H5202, Japan Industrial Standard, 2002. (In Japanese).